Projected Changes in Greater St. Louis Summer Heat Stress in NARCCAP Simulations

CLAIRE STEINWEG AND WILLIAM J. GUTOWSKI JR.

Department of Geological and Atmospheric Sciences, Iowa State University of Science and Technology, Ames, Iowa

(Manuscript received 21 August 2014, in final form 20 January 2015)

ABSTRACT

A matrix of four GCM–RCM combinations from the NARCCAP project is examined for changes in heat stress between contemporary and future scenario climates in the greater St. Louis region in Missouri. The analysis also compares the contemporary simulations with observation-based results from the North American Regional Reanalysis. The character of heat-stress days in one of the RCMs, the CRCM, tends to be like that of heat-stress days in the North American Regional Reanalysis, with high temperatures accompanied by high humidity. In contrast, heat-stress days in the other RCM, the Weather Research and Forecasting Model with Grell-Devenyi Cumulus Scheme (WRFG), have high temperature, but typically the humidity is similar to or even slightly drier than climatological values.

Although specific magnitudes of change differ between the simulations, all show a marked increase in projected heat stress, from a variety of perspectives. Increases in temperature contribute more to these increases than do increases in humidity, though both are relevant. All simulations agree that the frequency of excessive heat advisories and excessive heat warnings as defined by the National Weather Service could increase by midcentury, with multiple excessive heat advisories occurring every year. The day of first heat stress each summer could occur 3–4 weeks earlier as part of a more prolonged period when the region might experience heat stress each year. Although St. Louis has adopted measures to reduce health threats during heat-stress events, the measures consume human and economic resources; much more frequent and longer-lasting heat-stress events in the future have the potential to impose substantial costs on the region.

1. Introduction

One of the leading causes of weather-related mortality in the United States is extreme heat events (Kalkstein and Sheridan 2007), or heat waves. Although there is little physical destruction after an extreme heat event, as seen after a tornado or hurricane, the death toll may be as high (Smoyer 1998b). Extreme heat events can cause dehydration and dangerous increases in body temperature (Centers for Disease Control and Prevention 2013). The resulting stress can cause a wide range of effects: heatstroke; heat cramps; cardiovascular, respiratory, urinary, and neurological illness; and mortality (Smoyer 1998b). Deaths often increase more than 50% above baseline levels during extreme heat events.

Extreme heat events in recent years have received substantial attention, including the Chicago heat wave in 1995 (Semenza et al. 1996; Hayhoe et al. 2010) and the European heat wave in 2003 (WMO 2004; Kosatsky 2005). Urban areas in the central United States, in particular, have received substantial attention for impacts of heat waves on human mortality (Smoyer 1998a; Zanobetti and Schwartz 2008; Anderson and Bell 2011; Greene et al. 2011; Saha et al. 2014).

Heat waves have become more common, intense, and geographically widespread in recent years, and are expected to increase in the future (Kalkstein and Greene 1997; Meehl and Tebaldi 2004; Peng et al. 2010; Collins et al. 2014). The cost of heat stress in human lives, resources, and money, and the potentially increasing costs in the future require an understanding of how heat-stress events may change. Here we use projected climate changes from simulations for the North American Regional Climate Change Assessment Program (NARCCAP; Mearns et al. 2012, 2013) to assess potential changes in heat stress in the mid-twenty-first century for the greater St. Louis area in Missouri. NARCCAP is a multimodel project with a major motivation of providing regionally resolved projections for climate change vulnerability and impacts assessments.

Corresponding author address: William J. Gutowski Jr., Dept. of Geological and Atmospheric Sciences, Iowa State University of Science and Technology, 3021 Agronomy, Ames, IA 50011.
E-mail: gutowski@iastate.edu

DOI: 10.1175/WCAS-D-14-00041.1

Impacts analysis here is in terms of advisories and warnings issued by the U.S. National Weather Service, so that changes in heat stress are linked directly to efforts to inform response services and the general public of potentially hazardous weather.

St. Louis and the state of Missouri experienced a major heat wave in 1980, when 295 people died as a result of excessive heat; 114 of those were in St. Louis (C. Braun, Missouri Department of Health and Senior Services, 2011, personal communication). After that summer, Missouri implemented heat-warning systems that have helped to limit heat-related mortality. One safety measure against heat events in St. Louis is Operation Weather Survival, a network of organizations that work together to provide heat resources and education about heat events. The resources include heat advisory definitions, maps of cooling centers, plans for extreme heat, and organizations that will help during a heat event. Nonetheless, extreme heat continues to be an important health problem as evidenced by the 2012 extreme heat event that caused at least 18 deaths in the metropolitan area (National Weather Service 2012b). Also, although safety measures can limit mortality during a heat wave, they incur costs, so understanding how heat waves may change in the future remains important.

2. Methods

a. Apparent temperature

Multiple biophysical conditions such as temperature, humidity, wind speed, and solar radiation exacerbate heat-related health conditions (Steadman 1979a,b). In the United States, many National Weather Forecast offices issue extreme heat warnings based on temperature and humidity (e.g., National Weather Service 2012a). The apparent temperature, T_{app} (Steadman 1984), attempts to account for both. Term T_{app} is a measure of perceived temperature, incorporating human physiology and the body's ability to dissipate heat (Smoyer 1998b). It appears to be one of the better measures for activating heat-stress warnings (Zhang et al. 2014). Term T_{app} is typically calculated using daily 2-m air temperature (T_a) and relative humidity, or dewpoint (T_d). A good estimate (Smoyer 1998b) of apparent temperature is

$$T_{app} = 2.719 + 0.994(T_a) + 0.016(T_d)^2. \qquad (1)$$

We used T_a and specific humidity to compute T_d, and then used T_a and T_d to compute T_{app}.

There are two key thresholds used by the St. Louis National Weather Service for its weather advisory system (National Weather Service 2012a). The excessive heat advisory is when the apparent temperature is expected to reach 37.8°C (100°F) for four consecutive days or reach 40.6°C (105°F) on one day. The excessive heat warning is when the apparent temperature is expected to reach 40.6°C for four consecutive days. An excessive heat warning can also occur if the apparent temperature is expected to reach 43.3°C (110°F). Above the heat thresholds, the risk of heat illness increases rapidly (Smoyer 1998b). Consecutive days above critical thresholds compound problems, as populations experience sustained stress (Anderson and Bell 2011). During the 2003 European heat wave, for example, mortality in Paris increased markedly after the heat wave extended beyond about four days (Vandentorren and Empereur-Bissonnet 2005). Although a number of socioeconomic groups may suffer during heat waves (Reid et al. 2009; Chow et al. 2012; Harlan et al. 2013; Maier et al. 2014), the elderly are especially susceptible to sustained heat stress (Mirchandani et al. 1996; Bouchama and Knochel 2002; Basu and Ostro 2008; Fouillet et al. 2008; Sheridan et al. 2009).

b. Data sources

Data analyzed comes from two sources: the National Centers for Environmental Prediction (NCEP) North American Regional Reanalysis (NARR; Mesinger et al. 2006) and NARCCAP (Mearns et al. 2011, 2012, 2013). We use the NARR as our reference for observed behavior. NARCCAP is an international program that has created climate change projections at 50-km grid spacing for much of the United States, Canada, and northern Mexico. NARCCAP uses regional climate models (RCMs) with lateral boundary conditions given by output from global climate models (GCMs) or a global reanalysis, the NCEP–DOE AMIP-II reanalysis (Kanamitsu et al. 2002).

Our analysis uses two of the NARCCAP RCMs, the Canadian RCM (denoted CRCM in the NARCCAP archive) and the U.S. Weather Research and Forecasting Model with Grell-Devenyi Cumulus Scheme (denoted WRFG in the NARCCAP archive). Both simulated contemporary and future scenario climates using the National Center for Atmospheric Research Community Climate System Model (CCSM; Collins et al. 2006) and the Canadian Centre for Climate Modelling and Analysis CGCM3 (Scinocca and McFarlane 2004; Flato 2012). NARCCAP funding constraints limited the number of GCM–RCM combinations used for simulations (Mearns et al. 2012). These two RCMs were chosen because they form a compact subset of the NARCCAP ensemble of two RCMs driven by the same two GCMs. The simulations cover two periods: 1971–2000

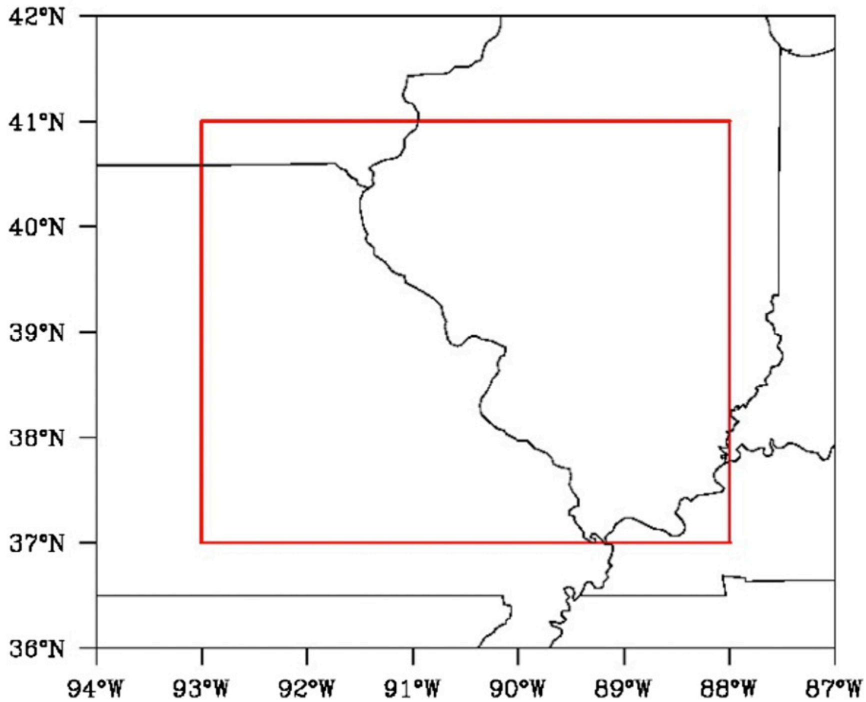

FIG. 1. Interior box is the map of the study area.

(contemporary) and 2041–70 (scenario). The future period uses the Special Report on Emissions Scenarios (SRES; Nakićenović and Swart 2000) A2 scenario, which is the second highest of the SRES emissions scenarios. For the future period simulated, global climate change is not sensitive to the specific SRES scenario used (Meehl et al. 2007), nor is the change substantially different from GCMs using newer scenarios (Collins et al. 2014). Further details of each model appear in Mearns et al. (2012, 2013).

We extracted daily NARCCAP and NARR output averaged over the greater St. Louis area (Fig. 1), defined here to be all grid points between 37°–41°N and 93°–88°W. The region has approximately 80 grid points from each regional model. Although the NARR output has finer grid spacing (32 km) than the RCMs, we assume that the small difference in resolution does not in itself yield substantial differences in averages over our analysis region. Using an analysis region surrounding St. Louis, rather than the grid box overlying the city, gives the analysis focus on the spatial scales directly simulated by the models and accounts for spatial shifts in simulated weather patterns. We use daily values because we analyze persistent weather behavior, not just an unusual occurrence during a day.

Note that these models do not include a detailed submodel to simulate directly urban climatology. Urban heat islands can enhance a regional warming in the core of a city (Zhou and Shepherd 2010; Li and Bou-Zeid 2013). By averaging over a larger area, the analysis focuses on heat stress over a broader region and, to some extent, minimizes the lack of explicit urban modeling in these RCMs.

c. *Analysis*

The analysis focuses on the period 1 May–31 August, which are the months that experience the greatest heat stress in the current climate, according to the NARR output (not shown). GCMs and RCMS may have temperature and humidity biases, so we used the apparent temperature from the NARR to correct RCM biases in the simulations. This allowed us to apply to all model output the National Weather Service's criteria for heat-stress advisories and warnings, which are based on T_{app}.

To obtain the correction, we first computed the May–August average T_{app} for the simulated contemporary climates and for the NARR output over a common period (1981–99). We treated the RCM–NARR difference (Table 1) as simulation bias and then subtracted this bias from all years in the contemporary and scenario RCM simulations. We thus assumed the bias does not change with climate change. More complex corrections are possible, such as quantile mapping of the simulated T_{app}, so that the T_{app} probability distribution functions (pdfs) for each contemporary simulation match the distribution of the observation-based T_{app} (e.g., Li et al. 2010;

TABLE 1. May–August average T_{app} (°C) for 1981–99, the RCM-NARR differences, and the interquartile range of T_{app} values, from the NARR and each of the simulations.

Model	Avg T_{app}	RCM-NARR	Interquartile range
NARR	31.10	—	9.27
CCSM–WRFG	29.19	−1.91	7.07
CGCM3–WRFG	27.59	−3.51	8.17
CCSM–CRCM	34.39	3.29	11.48
CGCM3–CRCM	30.70	−0.40	12.59

Berg et al. 2012). However, such correction would remove important features of the simulated pdfs, discussed below, that contribute to differences in results from each simulation and thus contribute to some of our understanding of the differences in projected changes in heat stress.

We use the adjusted T_{app} to calculate several statistics for heat events above the St. Louis National Weather Service's minimum threshold temperatures for an excessive heat advisory (37.8°C) and an excessive heat warning (40.6°C). Quantities computed include the following:

- Total heat-stress degree days (HSDD)—the sum of degrees on each day that exceed the critical thresholds (37.8° or 40.6°C)
- Total number of heat-stress days
- Number and average length of consecutive heat-stress days
- Number of heat-stress events of four consecutive days or longer
- Heat-stress intensity − HSDD/(number of heat-stress days)

We examine events lasting four or more days because such persistence helps trigger St. Louis National Weather Service heat advisories and warnings.

3. Results

a. Contemporary climate

Table 1 shows the model bias in T_{app} for the period with NARR output available. The WRFG model has a cool bias versus the NARR, whereas the CRCM has a small or positive bias. There is also similar sensitivity to the driving GCM: simulations using CCSM boundary conditions are warmer than simulations using the same RCM but CGCM3 boundary conditions. In addition, the CRCM simulations have a larger spread of values, as measured by their interquartile range, compared to the NARR output, whereas the WRFG simulations have a smaller range. The difference in range affects the heat-stress statistics of the two models.

Figure 2a shows the range of T_a values from each contemporary simulation and the NARR output for the overall climatology and for heat-stress days only. Note that these values are not bias corrected and so their distributions reflect the bias found in the uncorrected T_{app}. For all models and for the NARR, the large majority (>75%) of T_a values on heat-stress days fall within the upper quartile of their corresponding overall set of T_a values. Compared to the NARR, both models also show a slightly larger range of T_a values for days with heat stress. Figure 2b shows the same set of distributions but for T_d. For this variable, a marked difference occurs between models. For both CRCM simulations, T_d during heat-stress events tends to be among the more humid T_d values produced by the model. This behavior mimics the NARR results. In contrast, the WRFG T_d distributions during heat-stress events are approximately the same as the model's climatology. If anything, T_d is slightly drier during heat-stress events compared to climatology. Thus, the character of heat-stress events differs between WRFG and CRCM, with the latter behaving more like the NARR.

b. Climate change

Figure 3 shows the HSDD for contemporary and scenario climates for each simulation and for both thresholds. The climate change produces marked increases in HSDD. For the GCM–RCM combinations used here, the change is governed more by the RCM used than the GCM. This behavior is consistent with the analysis of summer temperature change for all NARCCAP GCM–RCM combinations by Mearns et al. (2013), who also find the RCM choice exerting greater influence on summer temperatures than the GCM choice. During summer in the central United States, atmospheric circulation is relatively weak compared to winter, and local processes such as land–atmosphere interactions and atmospheric convection play a greater role in determining regional climate. Thus, the RCM climates for the central U.S. in summer are not as strongly controlled by GCM boundary conditions as they are in winter.

The absolute changes in HSDD are greater for the CRCM simulations than the WRFG simulations. This is consistent with changes in mean temperature produced by these models for this region, with CRCM producing greater warming than WRFG for the same GCM boundary conditions (Mearns et al. 2013). However, the ratio of scenario versus contemporary HSDD is greater in the WRFG simulations for almost all GCM–RCM combinations and thresholds (Table 2). This is partly a consequence of WRFG producing fewer HSDD in the contemporary climate than CRCM. The behavior occurs because the frequency distributions of bias-corrected T_{app}

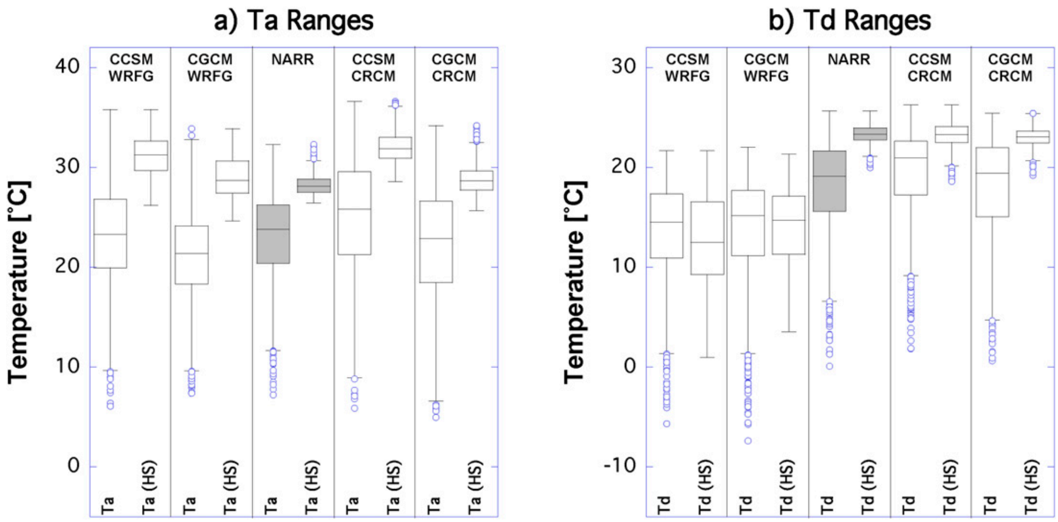

FIG. 2. Box-and-whisker diagrams giving ranges of temperature from the NARR and each contemporary climate simulation for all days (left diagram under each data source) and for heat-stress days (right diagram under each data source) for (a) near-surface air temperature and (b) dewpoint temperature. The horizontal lines on each box mark the 25th, 50th, and 75th percentile levels. The whiskers mark the extreme values or a range from the box equal to twice the interquartile range. For the latter, circles mark all values beyond the end of the whisker.

in the CRCM contemporary simulations cover a wider range of temperatures than do bias-corrected T_{app} in WRFG contemporary simulations: the standard deviation of temperatures during 30 years in the CRCM simulations (7.8° and 8.0°C, respectively) is greater than in the WRFG simulations (5.3° and 5.4°C, respectively). For comparison, the standard deviation of NARR T_{app} (6.6°C) falls between the two. The WRFG and CRCM standard deviations for just the NARR period are nearly the same as the 30-yr values above. The temperature distributions yield more days with heat stress in CRCM's contemporary climate than in WRFG's (Fig. 4). As with

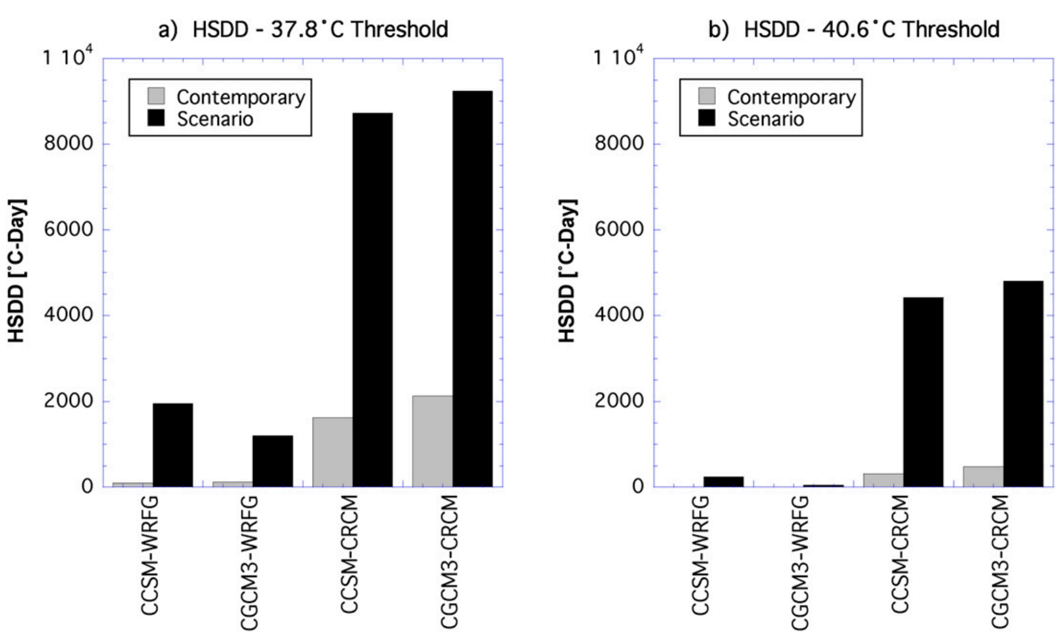

FIG. 3. Heat-stress degree days for (a) the 37.8°C heat advisory threshold and (b) the 40.6°C heat warning threshold for contemporary and scenario climates from each of the GCM–RCM combinations.

TABLE 2. Ratio of scenario to contemporary HSDD for both NWS critical thresholds (°C) from each GCM–RCM combination.

Model	Scenario/ contemporary 37.8°C	Scenario/ contemporary 40.6°C
CCSM–WRFG	20.32	718.51
CGCM3–WRFG	10.18	12.75
CCSM–CRCM	5.39	14.08
CGCM3–CRCM	4.34	10.07

HSDD, the number of days with heat stress increases markedly in all of the scenario climates, with absolute increases tending to be larger in the CRCM simulations.

The heat-stress intensity is the average number of heat-stress degree days on days that exceed one of the critical thresholds. The intensity of heat-stress events by this measure increases in the scenario climate for both thresholds (Fig. 5). However, the intensity does not increase by as large a factor as the HSDD. Rather, the scenario climates are characterized primarily by having more days above the critical thresholds rather than having substantially more intense heat-stress events. One result of this change is that days with heat stress appear earlier in the season in the scenario climates (Table 3). The CRCM results for the date of first heat stress are closer to the NARR results than are the WRFG results, which also have several years with no heat stress. WRFG's no-stress years are scattered throughout its contemporary simulations and so are not a clear consequence of the simulations starting in an earlier, perhaps cooler period than the NARR period. For all simulations, however, the date of first heat stress in the scenario climate is 3–4 weeks earlier than in the contemporary climate.

As discussed in section 2a, consecutive days exceeding either threshold are more important than an individual day with heat stress, as impacts on human health compound with increasing length of a heat-stress event. Figure 6 shows that the average length of consecutive-day events increases by roughly a factor of 2 for most simulations and thresholds, though not in all cases. In addition, the relative increase in average event length from contemporary to scenario climate is smaller than the relative increase in days that exceed either threshold. Thus, although the average length of a heat-stress event increases in the warmer climate, the large increase in HSDD is primarily due to an increase in the number of days that exceed one of the key thresholds rather than increasing length of heat-stress events.

The length of events, however, is important for determining changes in the frequency of excessive heat advisories and excessive heat warnings. Figure 7 shows the number of consecutive-day events lasting four or more days for each threshold. All simulations for the scenario climate give approximately three excessive heat advisories per year, though they differ substantially in the number of excessive heat advisories in the contemporary climate. Consistent with the results above, CRCM has more excessive heat advisories in its

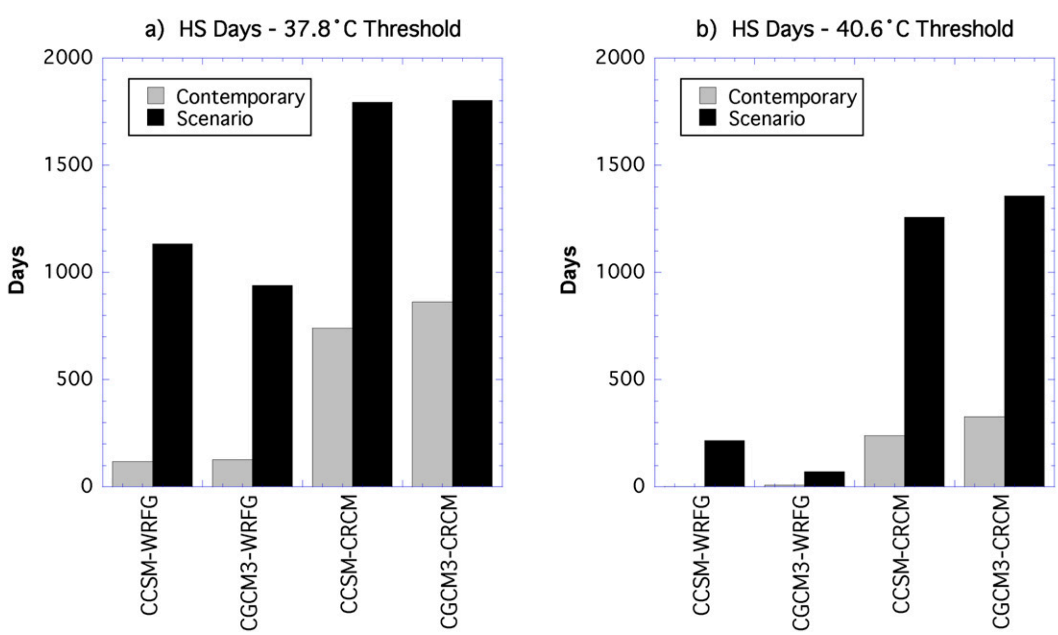

FIG. 4. Number of heat-stress days for (a) the 37.8°C heat advisory threshold and (b) the 40.6°C heat warning threshold for contemporary and scenario climates from each of the GCM–RCM combinations.

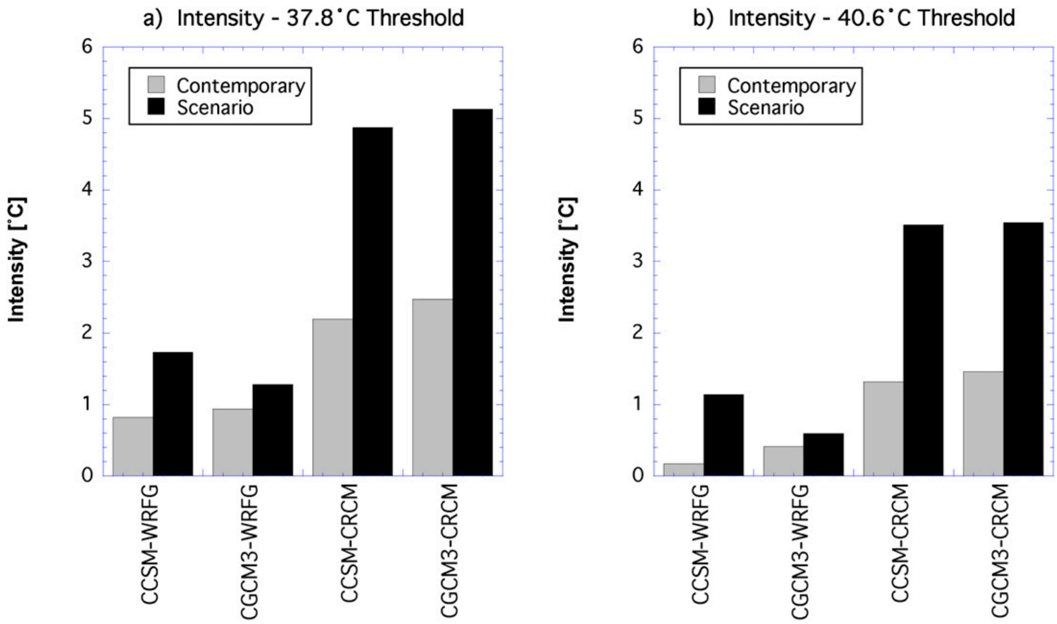

FIG. 5. Intensity of heat-stress days for (a) the 37.8°C heat advisory threshold and (b) the 40.6°C heat warning threshold for contemporary and scenario climates from each of the GCM–RCM combinations.

contemporary climates compared to WRFG and a smaller ratio of increase from contemporary to scenario climate.

Excessive heat warnings in the CRCM scenario simulations occur almost as frequently as the excessive heat advisories. In contrast, the CGCM3–WRFG combination produces no excessive heat warnings in either its contemporary or scenario climates. Excessive heat warnings do occur in the other WRFG set, but at a much lower frequency than in the CRCM simulations. The differing behaviors are at least partly a consequence of the wider distribution of T_{app} values in the CRCM simulations compared to WRFG simulations. They also result from the greater overall warming that occurs in this region in the CRCM simulations.

What contributes more to the increased heat-stress in scenario climates, more humidity or higher temperatures? Dewpoint temperature is especially relevant to consider for this evaluation, because it appears to be a good indicator of human comfort in warm, humid weather (Wallace and Hobbs 1977). Using (1),

$$\mathrm{dT_{app}} \approx 0.994\mathrm{dT}_a + 0.032T_d\mathrm{dT}_d \qquad (2)$$

gives the approximate change $\mathrm{dT_{app}}$ in terms of change in 2-m air temperature, dT_a, and change in dewpoint temperature, dT_d. For conditions near the critical thresholds, $0.032T_d \approx 1.2$, so the coefficients for dT_a and dT_d are approximately the same for the warmest, most humid conditions. For average May–August conditions, dT_d tends to be lower, so for average conditions, increases in dT_a contribute more to increases in average T_{app} than do increases in humidity as measured by dT_d (Table 4). The results suggest that warming plays a greater role than increasing humidity in causing more days to exceed critical apparent temperatures in the scenario climate.

4. Conclusions

We have examined a matrix of four simulations from the NARCCAP project for changes in heat stress between contemporary and future scenario climates in the greater St. Louis region. We have also compared the contemporary simulations with observation-based results from the North American Regional Reanalysis. Analysis shows that the character of heat-stress days in

TABLE 3. Average date of the first heat-stress day when a year has heat stress, using the 37.8°C threshold. Number in parentheses is the percentage of years with a heat-stress day. Note that the NARR results are for the common period 1981–99, whereas the climate model results are for the full period simulated for each climate.

Source	Contemporary	Scenario
NARR	24 Jun (100%)	—
CCSM–WRFG	5 Jul (79%)	13 Jun (100%)
CGCM3–WRFG	19 Jul (70%)	17 Jun (100%)
CCSM–CRCM	27 Jun (100%)	5 Jun (100%)
CGCM3–CRCM	26 Jun (100%)	5 Jun (100%)

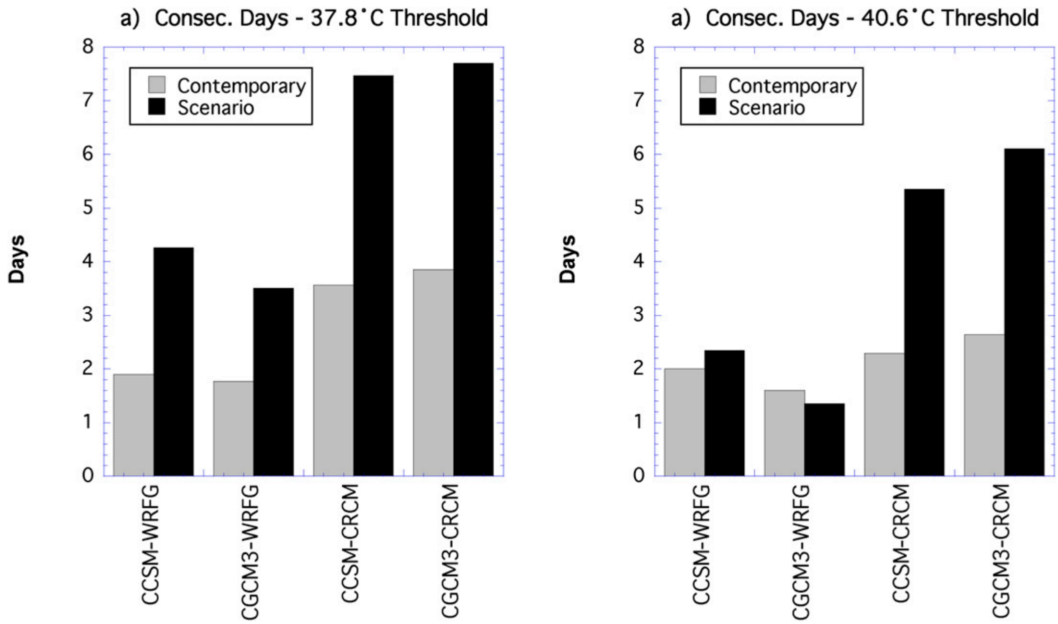

FIG. 6. Average consecutive days of heat stress for (a) the 37.8°C heat advisory threshold and (b) the 40.6°C heat warning threshold for contemporary and scenario climates from each of the GCM–RCM combinations.

the CRCM simulations tends to be more like that of heat-stress days in the NARR, with high temperatures accompanied by high humidity. The WRFG simulations, in contrast, have high temperature on heat-stress days, but typically the humidity is similar to or slightly drier than climatological distributions. Partly for this reason and partly because the WRFG temperature distribution tends to be narrower than the CRCM's temperature distribution, WRFG tends to have fewer heat-stress events in its contemporary climate than the CRCM, even after applying a bias correction.

We have performed analyses in terms of diagnostics that prompt advisories and warnings issued by the St. Louis National Weather Service (2012a), so that

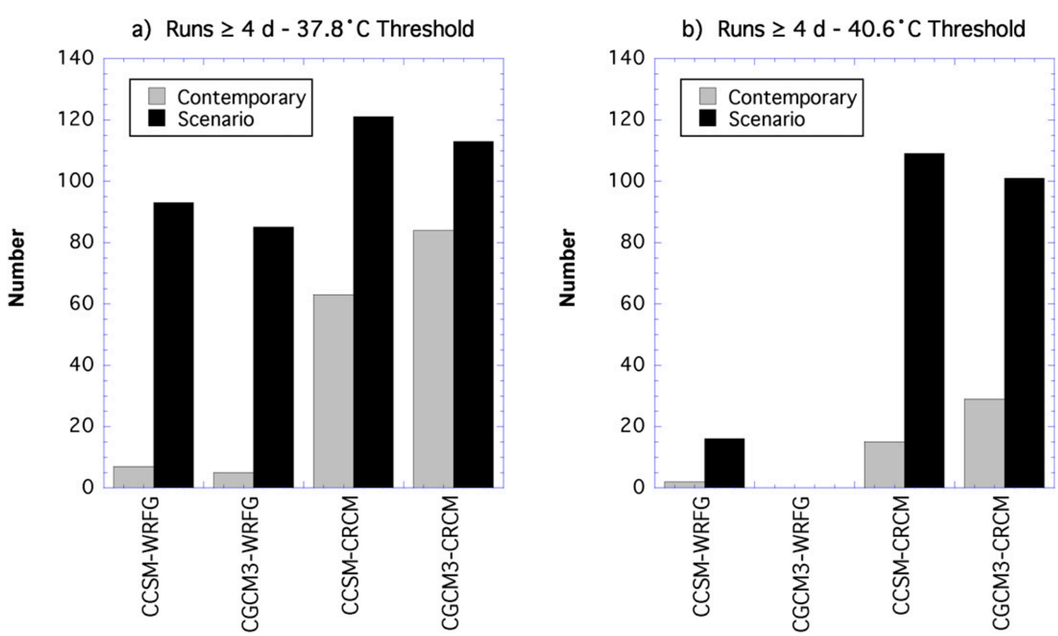

FIG. 7. Number of runs of four or more consecutive heat-stress days for (a) the 37.8°C heat advisory threshold and (b) the 40.6°C heat warning threshold for contemporary and scenario climates from each of the GCM–RCM combinations.

TABLE 4. Changes in average T_{app}, T_{app} change implied by (2) and contributions to (2); units: °C.

	T_{app} change	dT_{app} from (2)	0.994 dT_a	$0.032T_d dT_d$
CCSM–WRFG	3.33	3.32	2.80	0.52
CGCM3–WRFG	2.59	2.65	1.94	0.70
CCSM–CRCM	4.90	4.81	3.28	1.53
CGCM3–CRCM	4.65	4.52	3.10	1.42

changes in heat stress are linked directly to efforts to inform response services and the general public of potentially hazardous weather. Although specific magnitudes of change differ between the simulations, all show a marked increase in projected heat stress, from a variety of perspectives. Increases in temperature contribute more to these increases than do increases in humidity, though both are relevant. All simulations agree that the frequency of excessive heat advisories and excessive heat warnings could increase by midcentury, with multiple excessive heat advisories occurring every year. The day of first heat stress each summer could occur 3–4 weeks earlier as part of a more prolonged period when the region might experience heat stress each year.

St. Louis has adopted measures through its Operation Weather Survival to reduce threats to human health during heat-stress events, which could buffer impacts of their projected increases. However, such measures consume human and economic resources (e.g., White-Newsome et al. 2014), so much more frequent and longer-lasting heat-stress events in the future have the potential to impose substantial costs on the region. Furthermore, even when mitigation measures such as air conditioning are widely installed, the cost of expanding their use in a climate with much greater heat stress may become prohibitive to many (Sheridan 2007), thus increasing health risks.

Acknowledgments. This work was supported by National Science Foundation Grants ATM-0633567 and AGS-1243106, and the Iowa State University undergraduate Honors Program. We thank C. Uejio and the anonymous reviewers for their comments, which improved the manuscript. S. Kawazoe and B. Fisel provided invaluable computation support. We also thank the North American Regional Climate Change Assessment Program (NARCCAP) for providing the data we used. NARCCAP is funded by the National Science Foundation (NSF), the U.S. Department of Energy (DOE), the National Oceanic and Atmospheric Administration (NOAA), and the U.S. Environmental Protection Agency Office of Research and Development (EPA).

REFERENCES

Anderson, G. B., and M. L. Bell, 2011: Heat waves in the United States: Mortality risk during heat waves and effect modification by heat wave characteristics in 43 U.S. communities. *Environ. Health Perspect.,* **119,** 210–218, doi:10.1289/ehp.1002313.

Basu, R., and B. D. Ostro, 2008: A multicounty analysis identifying the populations vulnerable to mortality associated with high ambient temperature in California. *Amer. J. Epidemiol.,* **168,** 632–637, doi:10.1093/aje/kwn170.

Berg, P., H. Feldmann, and H.-J. Panitz, 2012: Bias correction of high resolution regional climate model data. *J. Hydrol.,* **448–449,** 80–92, doi:10.1016/j.jhydrol.2012.04.026.

Bouchama, A., and J. P. Knochel, 2002: Heat stroke. *N. Engl. J. Med.,* **346,** 1978–1988, doi:10.1056/NEJMra011089.

Centers for Disease Control and Prevention, cited 2013: Extreme heat and your health. [Available online at http://www.cdc.gov/extremeheat/.]

Chow, W. T. L., W.-C. Chuang, and P. Gober, 2012: Vulnerability to extreme heat in metropolitan Phoenix: Spatial, temporal, and demographic dimensions. *Prof. Geogr.,* **64,** 286–302, doi:10.1080/00330124.2011.600225.

Collins, M., and Coauthors, 2014: Long-term climate change: Projections, commitments and irreversibility. *Climate Change 2013: The Physical Science Basis,* T. F. Stocker et al., Eds., Cambridge University Press, 1029–1136, doi:10.1017/CBO9781107415324.024.

Collins, W. D., and Coauthors, 2006: The Community Climate System Model: CCSM3. *J. Climate,* **19,** 2122–2143, doi:10.1175/JCLI3761.1.

Flato, G. M., cited 2012: The third generation Coupled Global Climate Model (CGCM3). Environment Canada Canadian Centre for Climate Modelling and Analysis. [Available online at www.ec.gc.ca/ccmac-cccma/default.asp?lang=En&n=1299529F-1.]

Fouillet, A., and Coauthors, 2008: Has the impact of heat waves on mortality changed in France since the European heat wave of summer 2003? A study of the 2006 heat wave. *Int. J. Epidemiol.,* **37,** 309–317, doi:10.1093/ije/dym253.

Greene, S., L. S. Kalkstein, D. M. Mills, and J. Samenow, 2011: An examination of climate change on extreme heat events and climate–mortality relationships in large U.S. cities. *Wea. Climate Soc.,* **3,** 281–292, doi:10.1175/WCAS-D-11-00055.1.

Harlan, S. L., J. H. Declet-Barreto, W. L. Stefanov, and D. B. Petitti, 2013: Neighborhood effects on heat deaths: Social and environmental predictors of vulnerability in Maricopa County, Arizona. *Environ. Health Perspect.,* **121,** 197–204, doi:10.1289/ehp.1104625.

Hayhoe, K., S. Sheridan, L. Kalkstein, and S. Greene, 2010: Climate change, heat waves and mortality projections for Chicago. *J. Great Lakes Res.,* **36,** 65–73, doi:10.1016/j.jglr.2009.12.009.

Kalkstein, L. S., and J. S. Greene, 1997: An evaluation of climate/mortality relationships in large U.S. cities and the possible impacts of a climate change. *Environ. Health Perspect.,* **105,** 84–93, doi:10.1289/ehp.9710584.

Kalkstein, A. J., and S. C. Sheridan, 2007: The social impacts of the heat–health watch/warning system in Phoenix, Arizona: Assessing the perceived risk and response of the public. *Int. J. Biometeor.,* **52,** 43–55, doi:10.1007/s00484-006-0073-4.

Kanamitsu, M., W. Ebisuzaki, J. Woollen, S.-K. Yang, J. J. Hnilo, M. Fiorino, and G. L. Potter, 2002: NCEP–DOE AMIP-II

Reanalysis (R-2). *Bull. Amer. Meteor. Soc.,* **83,** 1631–1643, doi:10.1175/BAMS-83-11-1631.

Kosatsky, T., 2005: The 2003 European heat waves. *Eurosurveillance,* **10** (7). [Available online at http://www.eurosurveillance.org/ViewArticle.aspx?ArticleId=552.]

Li, D., and E. Bou-Zeid, 2013: Synergistic interactions between urban heat islands and heat waves: The impact in cities is larger than the sum of its parts. *J. Appl. Meteor. Climatol.,* **52,** 2051–2064, doi:10.1175/JAMC-D-13-02.1.

Li, H., J. Sheffield, and E. F. Wood, 2010: Bias correction of monthly precipitation and temperature fields from Intergovernmental Panel on Climate Change AR4 models using equidistant quantile matching. *J. Geophys. Res.,* **115,** D10101, doi:10.1029/2009JD012882.

Maier, G., A. Grundstein, W. Jang, C. Li, L. P. Naeher, and M. Shepherd, 2014: Assessing the performance of a vulnerability index during oppressive heat across Georgia, United States. *Wea. Climate Soc.,* **6,** 253–263, doi:10.1175/WCAS-D-13-00037.1.

Mearns, L. O., and Coauthors, cited 2011: The North American Regional Climate Change Assessment Program dataset. National Center for Atmospheric Research Earth System Grid Data Portal. [Available online at http://www.earthsystemgrid.org/project/NARCCAP.html.]

——, and Coauthors, 2012: The North American Regional Climate Change Assessment Program: Overview of phase I results. *Bull. Amer. Meteor. Soc.,* **93,** 1337–1362, doi:10.1175/BAMS-D-11-00223.1.

——, and Coauthors, 2013: Climate change projections of the North American Regional Climate Change Assessment Program (NARCCAP). *Climatic Change,* **120,** 965–975, doi:10.1007/s10584-013-0831-3.

Meehl, G. A., and C. Tebaldi, 2004: More intense, more frequent, and longer lasting heat waves in the 21st century. *Science,* **305,** 994–997, doi:10.1126/science.1098704.

——, and Coauthors, 2007: Global climate projections. *Climate Change 2007: The Physical Science Basis,* S. D. Solomon et al., Eds., Cambridge University Press, 747–845.

Mesinger, F., and Coauthors, 2006: North American Regional Reanalysis. *Bull. Amer. Meteor. Soc.,* **87,** 343–360, doi:10.1175/BAMS-87-3-343.

Mirchandani, H. G., G. McDonald, I. C. Hood, and C. Fonseca, 1996: Heat-related deaths in Philadelphia—1993. *Amer. J. Forensic Med. Pathol.,* **17,** 106–108, doi:10.1097/00000433-199606000-00004.

Nakićenović, N., and R. Swart, Eds., 2000: *Special Report on Emissions Scenarios*. Cambridge University Press, 570 pp.

National Weather Service, cited 2012a: Excessive heat briefing page. [Available online at http://www.crh.noaa.gov/lsx/?n=excessiveheatbriefing.]

——, cited 2012b: The historic 2012 heat wave. [Available online at http://www.crh.noaa.gov/lsx/?n=07_08_2012.]

Peng, R. D., J. F. Bobb, C. Tebaldi, L. McDaniel, M. L. Bell, and F. Dominici, 2010: Toward a quantitative estimate of future heat wave mortality under global climate change. *Environ. Health Perspect.,* **119,** 701–706, doi:10.1289/ehp.1002430.

Reid, C. E., M. S. O'Neill, C. J. Gronlund, S. J. Brines, D. G. Brown, A. V. Diez-Roux, and J. Schwartz, 2009: Mapping community determinants of heat vulnerability. *Environ. Health Perspect.,* **117,** 1730–1736, doi:10.1289/ehp.0900683.

Saha, M. V., R. E. Davis, and D. M. Hondula, 2014: Mortality displacement as a function of heat event strength in 7 US cities. *Amer. J. Epidemiol.,* **179,** 467–474, doi:10.1093/aje/kwt264.

Scinocca, J. F., and N. A. McFarlane, 2004: The variability of modeled tropical precipitation. *J. Atmos. Sci.,* **61,** 1993–2015, doi:10.1175/1520-0469(2004)061<1993:TVOMTP>2.0.CO;2.

Semenza, J. C., C. H. Rubin, K. H. Falter, J. D. Selanikio, W. D. Flanders, H. L. Howe, and J. L. Wilhelm, 1996: Heat-related deaths during the July 1995 heat wave in Chicago. *N. Engl. J. Med.,* **335,** 84–90, doi:10.1056/NEJM199607113350203.

Sheridan, S. C., 2007: A survey of public perception and response to heat warnings across four North American cities: An evaluation of municipal effectiveness. *Int. J. Biometeor.,* **52,** 3–15, doi:10.1007/s00484-006-0052-9.

——, A. J. Kalkstein, and L. S. Kalkstein, 2009: Trends in heat-related mortality in the United States, 1975–2004. *Nat. Hazards,* **50,** 145–160, doi:10.1007/s11069-008-9327-2.

Smoyer, K. E., 1998a: A comparative analysis of heat waves and associated mortality in St. Louis, Missouri—1980 and 1995. *Int. J. Biometeor.,* **42,** 44–50, doi:10.1007/s004840050082.

——, 1998b: Putting risk in its place: Methodological considerations for investigating extreme event health risk. *Soc. Sci. Med.,* **47,** 1809–1824, doi:10.1016/S0277-9536(98)00237-8.

Steadman, R. G., 1979a: The assessment of sultriness. Part I: A temperature–humidity index based on human physiology and clothing science. *J. Appl. Meteor.,* **18,** 861–873, doi:10.1175/1520-0450(1979)018<0861:TAOSPI>2.0.CO;2.

——, 1979b: The assessment of sultriness. Part II: Effects of wind, extra radiation and barometric pressure on apparent temperature. *J. Appl. Meteor.,* **18,** 874–885, doi:10.1175/1520-0450(1979)018<0874:TAOSPI>2.0.CO;2.

——, 1984: A universal scale of apparent temperature. *J. Climate Appl. Meteor.,* **23,** 1674–1687, doi:10.1175/1520-0450(1984)023<1674:AUSOAT>2.0.CO;2.

Vandentorren, S., and P. Empereur-Bissonnet, 2005: Health impact of the 2003 heatwave in France. *Extreme Weather Events and Public Health Responses,* W. Kirch, B. Menne and R. Bertollini, Eds., Springer, 81–88.

Wallace, J. M., and P. V. Hobbs, 1977: *Atmospheric Science: An Introductory Survey*. Academic Press, 467 pp.

White-Newsome, J. L., B. Ekwurzel, M. Baer-Schultz, K. L. Ebi, M. S. O'Neill, and G. B. Anderson, 2014: Survey of county-level heat preparedness and response to the 2011 summer heat in 30 U.S. states. *Environ. Health Perspect.,* **122,** 573–579.

WMO, 2004: World Meteorological Organization statement on the status of global climate in 2003. World Meteorological Organization, 12 pp.

Zanobetti, A., and J. Schwartz, 2008: Temperature and mortality in nine US cities. *Epidemiology,* **19,** 563–570, doi:10.1097/EDE.0b013e31816d652d.

Zhang, K., Y. Li, J. D. Schwartz, and M. S. O'Neill, 2014: What weather variables are important in predicting heat-related mortality? A new application of statistical learning methods. *Environ. Res.,* **132,** 350–359, doi:10.1016/j.envres.2014.04.004.

Zhou, Y., and J. M. Shepherd, 2010: Atlanta's urban heat island under extreme heat conditions and potential mitigation strategies. *Nat. Hazards,* **52,** 639–668, doi:10.1007/s11069-009-9406-z.